Solar-Terrestrial Physics. 2024. Vol. 10. Iss. 3. P. 121–136. DOI: 10.12737/stp-103202414. © 2024
N.V. Bakhmetieva, G.I. Grigoriev, I.N. Zhemyakov, E.E. Kalinina, A.A. Lisov. Published by INFRA-M Academic Publishing House

UDC 550.388.2, 551.510.536
DOI: 10.12737/stp-103202414

Received April 19, 2024
Accepted May 21, 2024

FEATURES OF EARTH'S LOWER IONOSPHERE DURING SOLAR ECLIPSE AND SUNSET AND SUNRISE HOURS ACCORDING TO MEASUREMENTS BY THE API METHOD NEAR NIZHNY NOVGOROD

N.V. Bakhmetieva
Radiophysical Research Institute
Lobachevsky State University,
Nizhny Novgorod, Russia, nv_bakhm@nirfi.unn.ru

G.I. Grigoriev
Radiophysical Research Institute
Lobachevsky State University,
Nizhny Novgorod, Russia, grig19@list.ru

I.N. Zhemyakov
Radiophysical Research Institute
Lobachevsky State University,
Nizhny Novgorod, Russia, ilia.zhem@yandex.ru

E.E. Kalinina
Radiophysical Research Institute
Lobachevsky State University,
Nizhny Novgorod, Russia, kalinina@nirfi.unn.ru

A.A. Lisov
Radiophysical Research Institute
Lobachevsky State University,
Nizhny Novgorod, Russia, lisov@nirfi.unn.ru

Abstract. We present the results of experimental studies into the response of Earth's lower ionosphere to a partial solar eclipse. The studies have been carried out using the method of resonant scattering of radio waves by artificial periodic irregularities (APIs) in ionospheric plasma. The irregularities were created in the field of a standing wave when a powerful radio wave, generated by radiation to the zenith by transmitters of the mid-latitude SURA heating facility, was reflected from the ionosphere. During location of a periodic structure by probe radio waves when the Wolf—Bragg backscattering condition was met, a scattered signal was received and its amplitude and phase were measured. After the end of the impact on the ionosphere, the irregularities gradually disappeared (relaxed). We have examined variations in characteristics of scattered signals. During the eclipse, the scattered signal amplitude increased by 30–40 dB, and the relaxation time increased 1.5–2.0 times. In some cases, stratification of the signal amplitude in the D-region was observed due to stratification of the electron density profile. By analyzing altitude profiles of relaxation time, we obtained neutral component temperature and density, height of the turbopause, and turbulent velocity. The velocity of vertical regular motion of plasma at each height was measured from the time variation in the scattered signal phase. From the results of measurements of scattered signal characteristics during four partial eclipses, we have obtained that the neutral component temperature decreases, on average, by 50–70 K. Variations in the temperature, vertical plasma velocity, and turbopause level exhibited deep quasi-periodic variations with periods from 15 min to several hours, typical of internal gravity wave propagation. The vertical temperature and velocity profiles showed changes with altitude on scales ranging from 5 to 30 km. Comparison between the results of studies of the lower ionosphere during sunrise-sunset hours has revealed that its response during a partial eclipse and the transition to the night regime is identical. According to the measurements by the partial reflection method, during the August 01, 2008 eclipse there was a decrease in the electron density in the D-region 3–5 times. We have concluded that during the eclipse there was a significant change in both the ionized and neutral components of the atmosphere in the lower ionosphere.

Keywords: ionosphere, plasma, neutral atmosphere, solar eclipse, sunrise, sunset, high-frequency heating, artificial periodic irregularities, temperature, vertical velocity, turbulence, internal gravity waves, SURA facility.

INTRODUCTION

A solar eclipse is one of the unique natural phenomena during which comprehensive changes occur in many atmospheric, ionospheric, and plasmaspheric parameters, which facilitates studying various processes in plasma and neutral atmosphere [Brunelli, Namgaladze, 1988; Lei J. et al., 2018; Dang et al., 2018]. During eclipses, properties of both the neutral and ionized components of the atmosphere change. During an eclipse, a decrease in the solar emission flux causes the atmosphere to cool, the electron density N_e in the D-region, E and F layers and the total electron content to decrease. Hundreds of papers have studied various aspects of the effect of solar eclipses on near-Earth space. The papers [Rishbeth, 1968; Belikovich et al., 2008; Huijun et al., 2009; Madhav, Manju, 2012; Kovalev et al., 2009; Chernogor, 2013; Manju et al., 2012] contain extensive bibliographies on this subject. Kovalev et al. [2009] have examined the effect of solar eclipses on ionospheric plasma, using data from mid-latitude vertical sounding stations, over the entire period from the beginning of ionospheric research in the USSR and Russia. The results of ionospheric observations from Tomsk Ionospheric Station during 28 solar eclipses with different

maximum phases from 1936 to 2007 have been summarized. Quantitative estimates of N_e variations in the E and F layers during solar eclipses were obtained.

A decrease in N_e in the F layer of the ionosphere was detected using the traditional vertical sounding method by analyzing ionograms [Rishbeth, 1968]. Later, rocket measurements of N_e were carried out [Kane, 1969] with incoherent scatter radars [Chernogor, 2013; Panasenko et al., 2019], satellites DEMETER, TIMED-SABER, ICON [Wang et al., 2008; Barad et al., 2022]; variations in absorption of HF and VLF radio waves in the lower ionosphere were treated by the radio astronomy method in a network of riometers [Bischoff, Taubenheim, 1967; Danilkin et al., 1961; Artem'eva et al., 1962]. Already the first rocket measurements showed a decrease in N_e by an order of magnitude in the D-region at altitudes 70–90 km during a total solar eclipse [Kane, 1969]. The incoherent scatter method found a decrease in electron temperature and a change of the direction of plasma stream from the plasmasphere [Chernogor, 2013; Akimov et al., 2002; MacPherson et al., 2000; Salah et al., 1986].

During eclipses in the F layer, the virtual reflection altitudes increased by 100 km or more with a delay to half an hour from the onset of the eclipse maximum phase [Belikovich et al., 2008; Chandra et al., 2007; Bamford, 2001]. Measurements of N_e by the partial reflection (PR) technique during the May 11, 1975 solar eclipse with a phase of 0.2 showed a decrease in N_e by 15−30 % at altitudes 75−80 km [Benediktov et al., 1978]. This technique also detected radio echoes at mesospheric heights during the eclipse — polar mesospheric summer echo (PMSE) lasting for ~4 min, which Tereshchenko et al. [2001] attributed to a fall in the temperature of the mesosphere. A number of papers have reported a sudden enhancement or appearance of a sporadic E_s layer during an eclipse [Sneva et al., 2013; Barad et al., 2022], the occurrence of F-spread phenomena, enhanced scattering of VHF and HF radar signals [Chandra et al., 2007]. Many studies have observed changes in geomagnetic variations (see, e.g., [Babakhanov et al., 2013; Ladynin et al., 2011]). Variations in the total electron content were examined by the radio scanning method from the results of reception of radio signals from artificial Earth satellites and global navigation systems GPS and GLONASS [Afraimovich et al., 1998; Tsai, Liu, 1999; Cherniak, Zakharenkova, 2018]. The same studies observed internal gravity waves generated by an eclipse as it occurs when the terminator (the boundary between light and shadow) passes through an observation point [Afraimovich et al., 2001; Akimov et al., 2002]. The LFM sounding method was employed to examine variations in maximum observable frequencies of radio lines during solar eclipses in a network of radio paths, to make model calculations in order to investigate the response of the ionosphere to a solar eclipse [Uryadov et al., 2000; Klimenko et al., 2007; Ivanov et al., 2012; Vertogradov et al., 2015].

Methods of ionospheric research are steadily improving; new methods are emerging, including those based on the impact of powerful high-frequency radio emission from heating facilities on the ionosphere. Among them, in particular, is the method of resonance scattering of radio waves by artificial periodic irregularities (APIs) of ionospheric plasma, which has proven to be effective in studying the ionosphere and the neutral atmosphere [Belikovich et al., 1999a, b; Belikovich et al., 2002]. The first results of the study into the D-region with APIs during the July 31, 1981 solar eclipse with a maximum phase of 0.75 are presented in [Belikovich et al., 1986; Belikovich, Goncharov, 1994]. New data on the response of the lower ionosphere to solar eclipses will make it possible to contribute to the research into its aeronomy and dynamics.

The purpose of this work is to generalize the results of observations of the effects of four partial solar eclipses on the lower ionosphere from a mid-latitude station near the heating facility SURA (56.1° N, 46.1° E), by analyzing characteristics of signals scattered by ionospheric plasma APIs.

1. GENERAL CHARACTERISTIC AND EXPERIMENTAL METHOD

For many years, methods based on the impact of powerful high-frequency radio emission on the ionosphere have been used to investigate the lower ionosphere. One of them is the method of measuring the key parameters of the ionosphere and the neutral atmosphere when it is disturbed by powerful radio waves generating APIs in ionospheric plasma. The method based on scattering of probe radio waves by APIs allows monitoring conditions of the lower ionosphere. The paper presents the results of ionospheric investigations during four partial solar eclipses from 1999 to 2022 by the method using the impact of emission from the powerful SURA heating facility generating APIs on Earth's ionosphere. The method of ionospheric research based on API generation is detailed in [Belikovich et al., 1999b; Belikovich et al. 2002; Bakhmetieva, Grigoriev, 2022]. It involves impacting Earth's ionosphere with powerful high-frequency radio emission. Uneven plasma heating in the field of a powerful standing wave generates the quasi-periodic structure of temperature and electron density having a spatial period Λ equal to half the length λ of a powerful radio wave. Sounding APIs by probe radio waves under the Bragg—Wolf backscattering condition and receiving scattered signals by dedicated equipment with amplitude and phase recorded make it possible to determine about ten most important characteristics of the ionosphere and the neutral atmosphere. Scattering of probe radio waves by APIs is resonance, i.e. a backscattered signal appears only when the waves scattered by individual irregularities are in phase. For the currently used frequencies 4–6 MHz of the impact on the ionosphere and effective radiated power of the heating facility to 120 MW, the relative disturbance of N_e in the irregularities may be $\Delta N/N \approx 10^{-4}$–$10^{-3}$ in the E layer and $\Delta N/N \approx 10^{-3}$–$10^{-2}$ in the D-region. Due to the resonance scattering, the signal-to-noise ratio in the lower ionosphere during the experiment was 10–100 [Belikovich et al., 1999b; Belikovich et al., 2002]. At present there are two methods of generating APIs — continuous and quasi-continuous heating. In the first

case, the heating facility is turned on for a few seconds to generate APIs (heating), and then is reset to pulse mode, emitting 30 μs short pulses (pause). As a result, the scattered signal amplitude and phase are measured during a pause in the operation of the heating facility. In the second case during heating, short pauses of 30 ms are made in which a short probe pulse 20–30 μs is emitted. As a result, it becomes possible to study the ionosphere not only during relaxation of irregularities, but also during their development [Bakhmetieva, Grigoriev, 2022; Bakhmetieva et al., 2023].

Figure 1, *a* schematically shows the generation of APIs during operation of the SURA heating facility in quasi-continuous mode and diagnostics of the ionosphere by probe pulses. Figure 1, *b* (left) illustrates the altitude and time dependence of scattered signal amplitude during the development and relaxation of APIs in the October 25, 2022 session, which started at 16:03:12 LT and lasted for 15 s. The signal amplitude at eight altitudes in the D-region, E and F layers and the interlayer E–F valley is shown on the right. Such visualization of a scattered signal in real time on the operator computer allows us to quickly adjust radiation parameters of the heating facility and the receiving system during the experiment.

The main characteristics of signals scattered by irregularities are their amplitude *A*, phase φ of the received signal and its relaxation time τ at the end of the impact on the ionosphere, defined by an e-fold decrease in the amplitude. The monographs [Belikovich et al., 1999b; Belikovich et al., 2002] detail the methods of measuring a number of parameters of the ionosphere and the neutral atmosphere and give some examples. For instance, the basis for determining the neutral component temperature and density, the turbopause level, and the turbulent velocity is the altitude dependence of the scattered signal relaxation time. Measuring its phase makes it possible to directly find the regular vertical plasma velocity, which is equal to the neutral component velocity (neutral wind velocity) since plasma in the lower ionosphere is a passive admixture and moves along with a neutral medium [Gershman, 1974].

The paper presents and discusses the results of the study of the lower ionosphere during four partial solar eclipses. The method of impacting the ionosphere involves both continuous and quasi-continuous heating. In different experiments, the frequencies of the impact on the ionosphere, the radiated power, and the powerful radio wave polarization differed. Raw data was processed by a single algorithm. The corresponding references are given in the text.

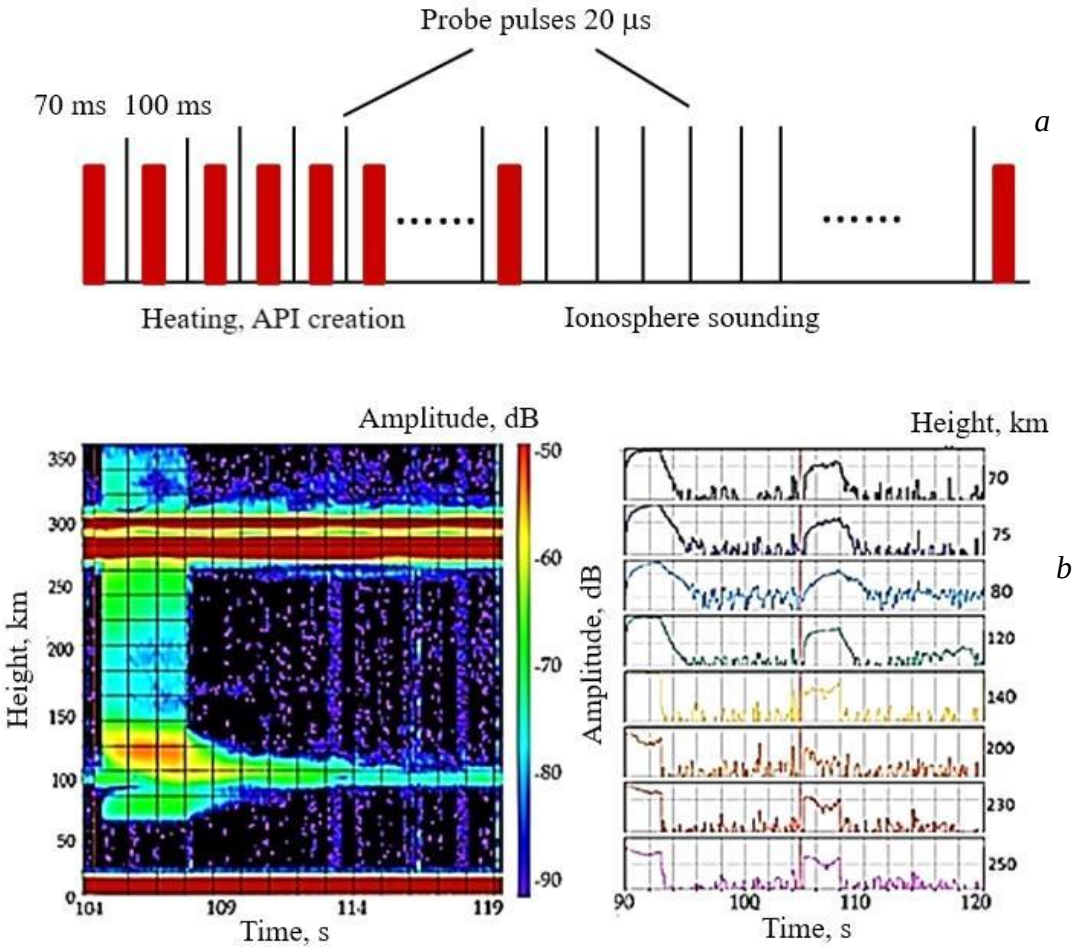

Figure 1. Generation of APIs during quasi-continuous operation of the SURA heating facility and diagnostics of the ionosphere with probe pulses (*a*); scattered signal amplitude (*b*) as a function of altitude and time during the development and relaxation of irregularities in the session that started at 16:03:12 on October 25, 2022 and lasted for 15 s (left); signal amplitude at eight altitudes in the D-region, E and F layers (right)

APIs were generated by SURA transmitters (56.13° N; 46.10° E, Vasilsursk village) emitting a powerful radio wave to the zenith, which generally has extraordinary polarization at frequencies of 4.30, 4.75, or 5.60 MHz. The receiver was at a distance of 1 km from the heating facility. General characteristics of the four solar eclipses are presented in Table 1. All these eclipses with close magnitudes of the maximum phase occurred in the afternoon, Moscow time, mainly during low geomagnetic activity. The August 11, 1999, March 20, 2015, and October 25, 2022 eclipses took place during the rise phase of solar activity; and the August 01, 2008 eclipse, in the year of its minimum.

The date and time of the onset of the eclipse T_1, the maximum phase T_2, the end T_3, as well as heliogeophysical parameters during this period are listed: the sunspot number W, the radio emission flux $F10.7$, the geomagnetic indices K_p and A_p [http://www.wdcb.ru/stp/index.ru.html].

Some of the above results have been discussed in [Bakhmetieva et al., 2016, 2017]. During the observations, the ionosondes Basis and CADI were always in operation. When recording an ionogram, the SURA facility was turned off. In addition, we have used data from the ionosonde Parus (IZMIRAN), which is in the public domain [https://www.izmiran.ru/ionosphere/moscow/].

Table 1

Date	LT			Eclipse phase	W	$F10.7$, s.f.u.	K_p	A_p, nT
	T_1	T_2	T_3					
Aug. 11, 1999	14:07	15:15	16:21	0.608	97.3	1708	1–2	4–7
Aug. 01, 2008	13:07	14:15	15:21	0.653	0.5	663	0–1	4
Mar. 20, 2015	12:22	13:34	14:36	0.618	64	1263	3	22
Oct. 25, 2022	12:30	13:44	14:57	0.757	59.2	1194	1	3

2. VARIATIONS IN PARAMETERS OF THE LOWER IONOSPHERE AND THE NEUTRAL ATMOSPHERE DURING SOLAR ECLIPSES

Let us present the main results of the study of the lower ionosphere, obtained by the API method, for each eclipse. We focus on neutral component variations.

The August 11, 1999 eclipse

The partial solar eclipse near Vasilsursk village began at 14:07 LT, reached the maximum phase of 0.608 at 15:15 LT, and ended at 16:21 LT (LT=UT+4). The eclipse occurred during high solar activity; the geomagnetic field was slightly disturbed, K_p=1−2. The experiments were carried out on August 10−12, 1999 from 9 to 17 LT. The F-layer critical frequencies on these days varied from 6.6 to 7.7 MHz at the beginning of measurements, decreasing to 5.6–6.5 MHz by 17:00 LT. On the day of the eclipse on August 11, 1999, 10 min after its onset, the frequencies f_oF2 began to decrease, reaching minimum values of 6.0 MHz by the maximum phase, and remained constant for 20 min. After the maximum phase of the eclipse, the F layer gradually recovered. The corresponding decrease in N_e at the maximum of the F layer was 26 %. On test days, the f_oF2 variation correlated with the usual daytime daily course. For the E layer, f_oE=3.6−3.8 MHz. During the maximum phase, f_oE, equal to 3.7 MHz before the eclipse, decreased by 0.8–0.9 MHz. The E_s layer with f_oE_s=4−4.5 MHz, which occasionally increased to 6−8 MHz, was observed almost constantly in those days.

With continuous heating, each measurement session lasted for 15–20 s. During the first 3 s, the ionosphere was heated by a radio wave of extraordinary polarization at a frequency f=5.75 MHz with an effective power of 130 MW on August 10, 1999 and 60 MW in the following days. The 3 s heating was followed by a 12–17 s pause during which 20−50 μs probe pulses of the same frequency and a repetition rate of 50 to 100 Hz were emitted. Quadrature components of the scattered signal were detected which were used to determine its amplitude and phase.

Scattered signal characteristics

During the August 11, 1999 partial solar eclipse, a complex nonuniform structure of scattered signals was observed. Figure 2 exemplifies altitude-time variations in scattered signal amplitude during the August 11, 1999 eclipse (*a*) and on August 12, 1999 (*b*). Shown here is the characteristic appearance of scattered signals in the D-region at altitudes 57–85 km and in the E layer at 90–140 km. During the eclipse, pronounced scattered signal turbulization is seen to occur in the E layer. This is reflected in the fact that during altitude and temporal recordings of scattered signal amplitude, such as those shown in Figure 2, there are stratifications in the E layer and in the upper part of the D-region, associated, as observed in monographs [Belikovich et al., 1999b; Belikovich et al., 2002], with stratifications in the vertical profile $N_e(h)$. These stratifications may be natural, as we have repeatedly observed in experiments on the study of the ionosphere by the PR and API methods. In addition to the stratifications of $N_e(h)$, signals of this type may be related to the interference of signals scattered by APIs, sporadic layers, and large-scale irregularities of natural origin. As a result, the received signal phase may be noticeably distorted, which makes it difficult and sometimes impossible to measure the vertical plasma velocity and hence the neutral component [Belikovich et al., 1999b; Belikovich et al., 2002]. The scattered signal amplitude in the D-region and E layer during the eclipse increased by 15–20 dB as compared to the previous day. Figure 2, *b* also exemplifies the development of the E_s layer at altitudes 134–137 km in the 16:06:14 session and at 112–123 km in the 14:10:13 session on the day after the eclipse, August 12, 1999. Note that the method based on resonance scattering of probe radio waves by APIs

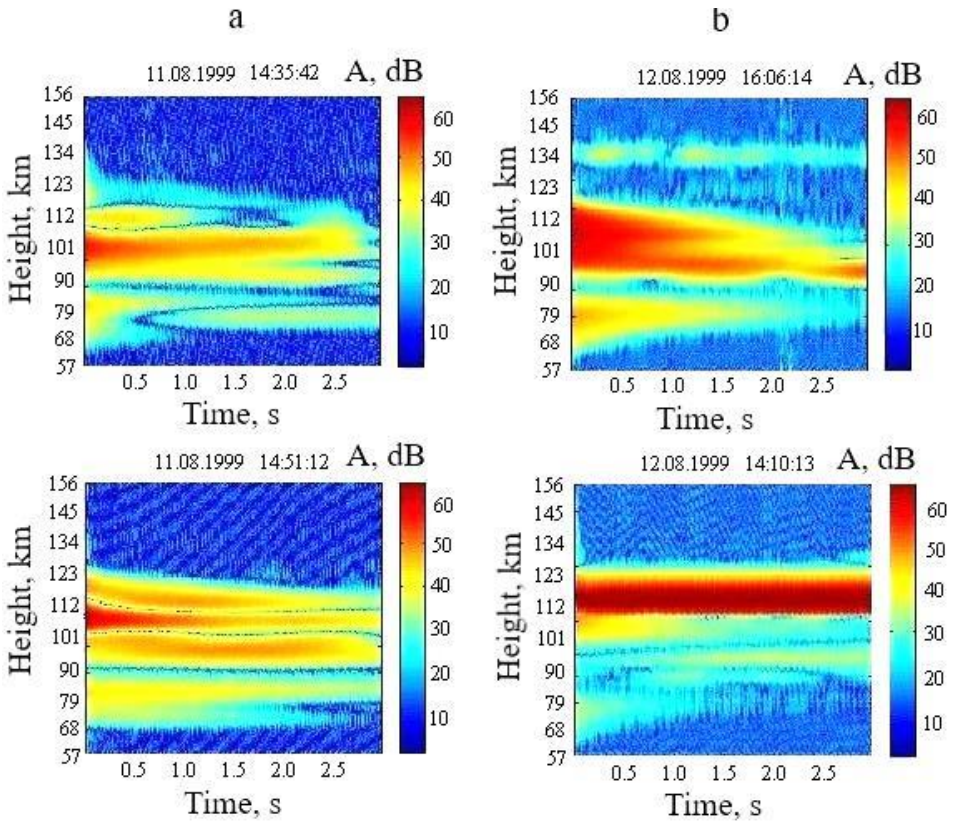

Figure 2. Height-time variations in scattered signal amplitude on the day of the eclipse, August 11, 1999, (*a*) and on the next day, August 12, 1999, (*b*). Shown here is the turbulence of the lower ionosphere during the August 11, 1999 eclipse and the development of the E_s layer at heights 134–137 km and 112–123 km on August 12, 1999

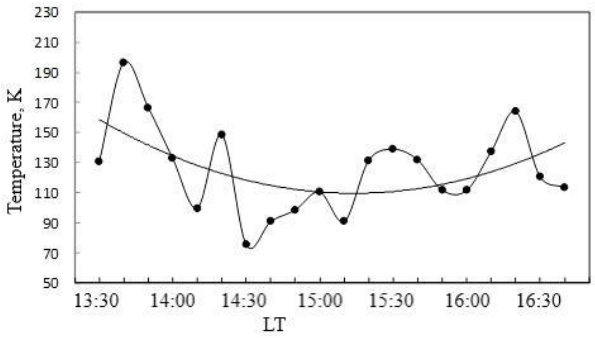

Figure 3. Temperature variations at 101–103 km during the August 11, 1999 eclipse from 13:30 to 16:30 LT. Each point was obtained by averaging over 10 min and assigned to the beginning of the time interval. The second-order polynomial trend line is also plotted. During the eclipse, the temperature dropped, on average, by 50–70 K

allows us to detect the weakest sporadic layers inaccessible to ionosondes [Kagan et al., 2005; Bakhmetieva et al., 2010].

Natural large-scale turbulence in the mesosphere and intense reflections in the range of virtual altitudes 125–140 km from the semitransparent E_s layer 5–15 km thick were often observed during the eclipse. Above the E-layer maximum at 130–140 km, reflections were sometimes recorded which represented a scattered signal from a weak semitransparent E_s layer (see Figure 2, *b* for August 12, 1999; the start time of the session is 16:06:14).

Temperature of the neutral atmosphere

During an eclipse, the atmosphere should cool and the thermospheric temperature should go down. The neutral component temperature was determined from the height dependence of the relaxation time with the algorithm [Tolmacheva, Belikovich, 2004]. Figure 3 illustrates temperature variations on the day of the eclipse, August 11, 1999, from 13:30 to 16:30 LT at heights 101–103 km. Each temperature value was derived by averaging over 10 min and was assigned to the beginning of the time interval. During the eclipse, the temperature at these heights of the lower thermosphere dropped, on average, by 50–70 K. On the day of the eclipse, the decrease in the neutral component temperature was masked by intense wave activity. This has to be taken into account when analyzing the effect of the eclipse on the temperature regime of the thermosphere. On this day, there were strong temperature variations with periods of 120, 60, and 20 min, caused by propagation of internal gravity waves (IGWs) [Tolmacheva, Belikovich, 2004]. The results of measurements by the API method on the test days, August 10, 1999 and August 12, 1999, have shown, however, that IGWs of the same periods were observed during the entire three-day measurement cycle. Notice that irregular phenomena in the ionosphere hamper the determination of the neutral atmosphere temperature by the API method. A positive point is a decrease in the absorption of both a powerful wave generating irregularities and a probe wave during

the eclipse, which provides an increase in the scattered signal amplitude and reduces the temperature measurement error, which under normal conditions is within 10–15 % [Belikovich et al., 1999b; Belikovich et al., 2002; Tolmacheva, Belikovich, 2004]. Tolmacheva and Belikovich [2004] have reported the results of determination of the atmospheric density at heights of 106 and 108 km on August 10–12, 1999 from 10 to 17 LT. It is shown that on the day of the eclipse and in the following days there were 60-min density variations and 17–25 % relative variations of parameters. Generation of atmospheric waves during an eclipse is well known and has been repeatedly observed by various methods [Chernogor, 2013; Dang et al., 2018; Panasenko et al., 2019; Bakhmetieva et al., 2021].

During the same period on August 11, 1999 in France, where the solar eclipse was total, atmospheric pressure variation on Earth and in N_e in the ionosphere were measured. Data from microbarograph stations and ionosonde networks was obtained. The measurements revealed wave-like pressure variations the authors attributed to IGW generation by a probable source in the lower atmosphere and in the thermosphere. In the lower atmosphere, the wave period was 12 min; and in the thermosphere, ~60 min [Farges et al., 2003].

Vertical profiles and time variations in the vertical plasma velocity revealed 20 s deep and rapid variations from session to session. In the E layer, the velocity varied from –10 to +8 m/s (negative values correspond to upward motion). The greatest variations in instantaneous velocity were recorded at heights from 90 to 110 km, where in many sessions the velocity changed sign, i.e. the direction of plasma motion with possible formation of E_s layer [Gershman, 1974; Whitehead, 1989; Mathews, 1998]. Bakhmetieva et al. [2001] present values of the altitude vertical velocity gradient from 10^{-4} to $8 \cdot 10^{-3}$ s^{-1}, sufficient for plasma redistribution and formation of E_s layer due to wind-induced redistribution of ionization [Gershman et al., 1976].

The August 01, 2008 eclipse

A partial solar eclipse near Vasilsursk village began at 13:07 LT, had a maximum magnitude of 0.653 at 14:15 and ended at 15:21. Ionospheric conditions were analyzed from July 30 to August 2, 2008 simultaneously by two methods: by the PR method with recording of characteristics of the signals scattered by natural irregularities of the D-region, and by the method of generating APIs with measurement of the amplitude and phase of the signals scattered by them [Bakhmetieva et al., 2016]. On those days there were no geomagnetic disturbances, $K_p \leq 1$. According to ionosonde data, f_oE=2.8÷3.3 MHz, f_oF1=3.4÷4 MHz, and f_oF2=4.5÷4.9 MHz at solar minimum. The E_s layer was observed with a screening frequency of 2.8 MHz and a maximum reflection frequency to 3.5 MHz.

The originality of this experiment was that every minute for 10 s signals scattered by APIs were recorded, and for the next 50 s signals of partial reflections from natural irregularities of the D-region were detected. The transmitter for partial reflections operated at a frequency of 2.95 MHz; both magnetoionic components of the signal scattered by D-region irregularities were received. APIs were generated by radio waves of extraordinary polarization from SURA transmitters at a frequency of 4.7 MHz with an effective power of 80 MW. As a result, the PR technique provided vertical profiles of N_e in the D-region of the ionosphere at heights of 70 to 85 km; the measurement technique is detailed in [Belikovich et al., 2003a, 2008]. Using the API method, we obtained height-time dependences of scattered signal amplitude, relaxation time, and phase, as well as vertical plasma velocity at 60–120 km. The combination of the PR and API methods made it possible to cover almost the entire height range of the lower ionosphere. Height-time variations in signals scattered by natural irregularities, their variations correlating with the passage of the moon's shadow across the solar disk were analyzed. Some results of these measurements are presented in [Bakhmetieva et al., 2017].

The lower ionosphere during the August 01, 2008 eclipse

Visualization of measurements provides a visual representation of a change in ionospheric conditions during an eclipse. Figure 4, taken from [Bakhmetieva et al., 2017], illustrates height-time dependences of the amplitude of signals of ordinary (top panel) and extraordinary (middle panel) probe radio waves with a frequency of 2.95 MHz, which are scattered by N_e natural irregularities of the D-region, and signals specularly reflected from ionospheric layers. The bottom panel shows variations in the amplitude of radio waves of extraordinary polarization with a frequency of 4.7 MHz, which are scattered by APIs. Arrows indicate the times of the beginning, maximum phase, and end of the eclipse. In the top and middle panels are scattered signals of partial reflections in the D-region in the height range of 70 to 95 km. The ordinary wave was first reflected at heights from 100 km to 150 km with multiple reflections from the E and F layers. The E_s layer was observed during the entire measurement period. During the eclipse, the virtual reflection height of the extraordinary wave in the E layer increased by ~20 km, and the ordinary radio wave gradually began to be reflected in the F layer at more than 250 km.

In the D-region, N_e was found by the differential absorption method [Belikovich et al., 2003a]. This yielded that during the eclipse N_e in the D-region decreased 3–5 times. It is also shown that N_e in the lower D-region reaches minimum values almost at the moment of the maximum phase of the eclipse, and above 85–90 km it is delayed by 22–25 min, which may be due to different recombination laws in the lower and upper part of the D-region [Belikovich et al., 2003a]. At the same time there were wave-like variations in N_e with a well-defined period of 45 min, and traces of traveling disturbances in vertical sounding ionograms. Note that the results of measurements by the PR technique during the August 01, 2008 eclipse generally accord well with the simultaneous observations of the March 29, 2006 partial solar eclipse with a maximum phase of 0.696 in the middle (Vasilsursk village) and high (Loparskaya village) latitudes by this technique [Belikovich et al., 2003a, 2008].

The API method recorded intense scattered signals from 70 km in the D-, E-, and F-regions. As the eclipse evolved, the amplitude of the signal scattered by irregularities gradually decreased and APIs stopped forming 45 min after the beginning of the eclipse even before the onset of its maximum phase (see Figure 4). This is due to the fact that the extraordinary component of a powerful 4.7 MHz wave whose emission generated irregularities ceased to be reflected from the ionosphere in response to a general decrease in N_e and hence a decrease in f_oF2 to 3.0–3.2 MHz. Thus, we did not manage to examine variations in the amplitude and relaxation time of the signal scattered by irregularities, as well as to estimate the atmospheric temperature and the plasma velocity during the eclipse due to natural factors. Twenty minutes before the end of the eclipse, reflections from the F2 layer occurred; and 7 min later, signals scattered by APIs in the D- and E-regions appeared.

Measurements of the scattered signal phase have revealed that before and after the eclipse, there were variations in the vertical plasma velocity to 10 m/s with periods typical of IGWs.

The March 20, 2015 eclipse

The partial solar eclipse on March 20, 2015 occurred from 12:22 to 14:36 with a maximum phase of 0.618 at 13:34 Moscow winter time (LT=UT+3). The ionosphere was investigated by the method of resonance scattering of radio waves by APIs on March 16–21 from 10 to 16 LT. At that time, there was an increase in geomagnetic activity followed by a planetary-scale magnetic storm with K_p to 8, which developed by noon on March 17, 2015. The magnetic storm was preceded by a solar flare on March 15, 2015, which occurred with a large coronal mass ejection. The magnetic storm lasted for more than a day, and on March 19, 2015 magnetic activity returned to the prestorm level with K_p=1÷3. On the day of the eclipse, f_oF2 increased to 9 MHz; f_oF1, to 4.7 MHz; and f_oE, to 3.5 MHz. At ~100 km, the E_s layer was recorded with a maximum reflection frequency to 3.5–4.0 MHz. During the measurements, multiple traveling disturbances were found in vertical sounding ionograms.

Figure 5, *a*, *b* illustrates the height-time dependence of the amplitude of a signal, scattered by irregularities, and the vertical plasma velocity in the lower ionosphere. Shown here are signals scattered by APIs in the D-region (65–86 km), in the E layer (90–130 km), and in the E_s layer (100–115 km). About an hour before the eclipse, scattered signals appeared at 84–88 km, which had not been observed before. There is a pronounced expansion of the altitude range of scattered signals (the range of API formation) in the E layer and an increase in the initial height of signal detection in the D-region.

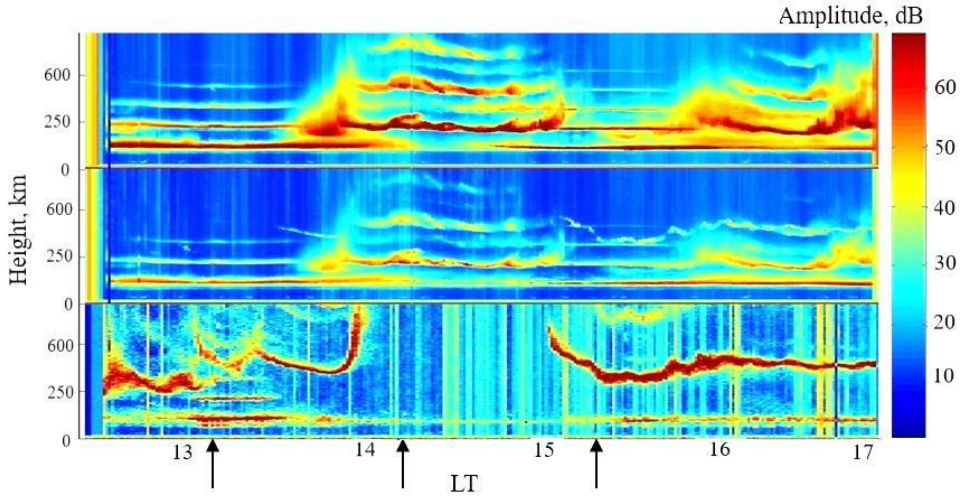

Figure 4. Ionospheric response to the August 01, 2008 partial solar eclipse as inferred from complex recording of scattered signals by the partial reflection technique and the method of resonance scattering by APIs. The top and middle panels show a scattered signal from the D-region at a frequency of 2.95 MHz for ordinary and extraordinary modes respectively; the lower bottom exhibits a signal scattered by API at a frequency of 4.7 MHz

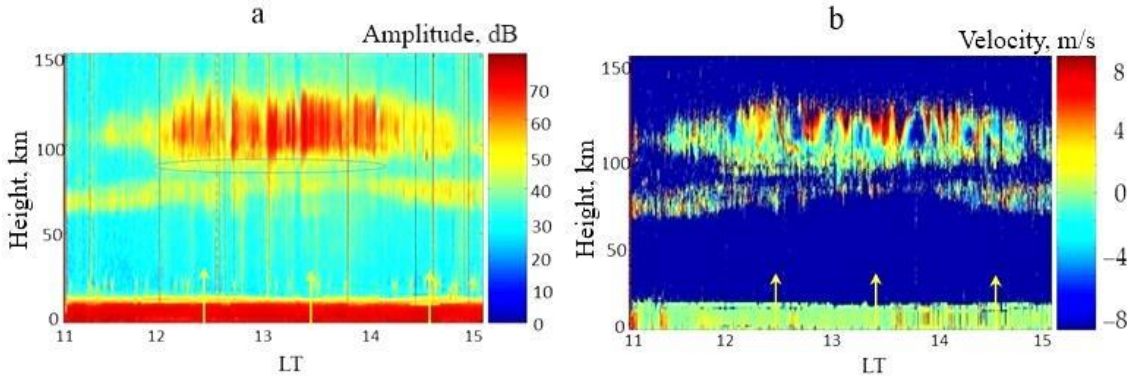

Figure 5. Height-time dependence of scattered signal amplitude (*a*) and vertical plasma velocity (*b*) in the D- and E-regions of the ionosphere during the March 20, 2015 partial solar eclipse

Features of height-time variations in scattered signal amplitude and relaxation time

Over time, during the eclipse the scattered signal amplitude increased by 30–40 dB in the E layer.

The amplitude increase, which began about an hour before the eclipse, intensified significantly during it. The most likely reason for this is a decrease in absorption due to a general decrease in N_e with decreasing ionizing emission from the Sun. The signals scattered by APIs in the E layer gradually began to occupy an increasing range of heights. The same effect is seen in Figure 6, which illustrates time variations in averaged vertical profiles of amplitude and relaxation time of a signal, scattered by API, for nine 5-min measurement sessions during the March 20, 2015 eclipse. The profiles were obtained by averaging the data over a 5-min interval. There is an increase in the amplitude of the scattered signal in the E layer and an increase in the relaxation time in the D-region. Such a time variation in scattered signal amplitudes in the D-region corresponds to a gradual transition to the nightside ionosphere, similar to sunset and sunrise phenomena [Belikovich, Benediktov, 1986, 2002; Belikovich et al., 2000; Bakhmetieva et al., 2005]. Note also that the scattered signals in the D-region at the beginning of observations and after the end of the eclipse often had an amplitude higher than the signals scattered by irregularities in the E layer, although scattered signals in the D-region generally have an amplitude lower by 20–30 dB. Furthermore, the lower boundary of API formation in the D-region increased during the eclipse, which corresponds to a change in the vertical N_e profile [Belikovich et al., 1999b; Belikovich et al., 2002]. Profiles in the middle panel of Figure 6 indicate that the lower boundary of the D-region rises and a scattered signal appears at heights 84–88 km. For an hour near the maximum phase of the eclipse, there was a stratification of the scattered signal amplitude in the D-region. A similar effect was observed during pre-sunset hours on June 15, 2001 and was associated with stratification of the N_e profile [Belikovich et al., 1999b; Belikovich et al., 2002; Belikovich, Benediktov, 2002].

During the eclipse, the scattered signal amplitude and relaxation time increased. Figure 7 exhibits time dependences of scattered signal amplitude (solid line) and relaxation time (dashed line) for 88 km (*a*) and 100 km (*b*). The scattered signal amplitude is seen to increase significantly during the eclipse (30–40 dB in the E layer and to 20 dB in the D-region). The largest amplitude increase was recorded near the maximum phase. The scattered signal relaxation time increased approximately 1.5–2 times.

An important ionospheric effect during the eclipse was the appearance of a scattered signal an hour before the eclipse at 84–88 km, which is clearly seen in Figures 5, 6. The scattered signal that appeared at these heights relaxed relatively slowly — the relaxation time in some sessions exceeded 4–5 s versus usual 1–2 s typical of the D-region [Belikovich et al., 1999b; Belikovich et al., 2002].

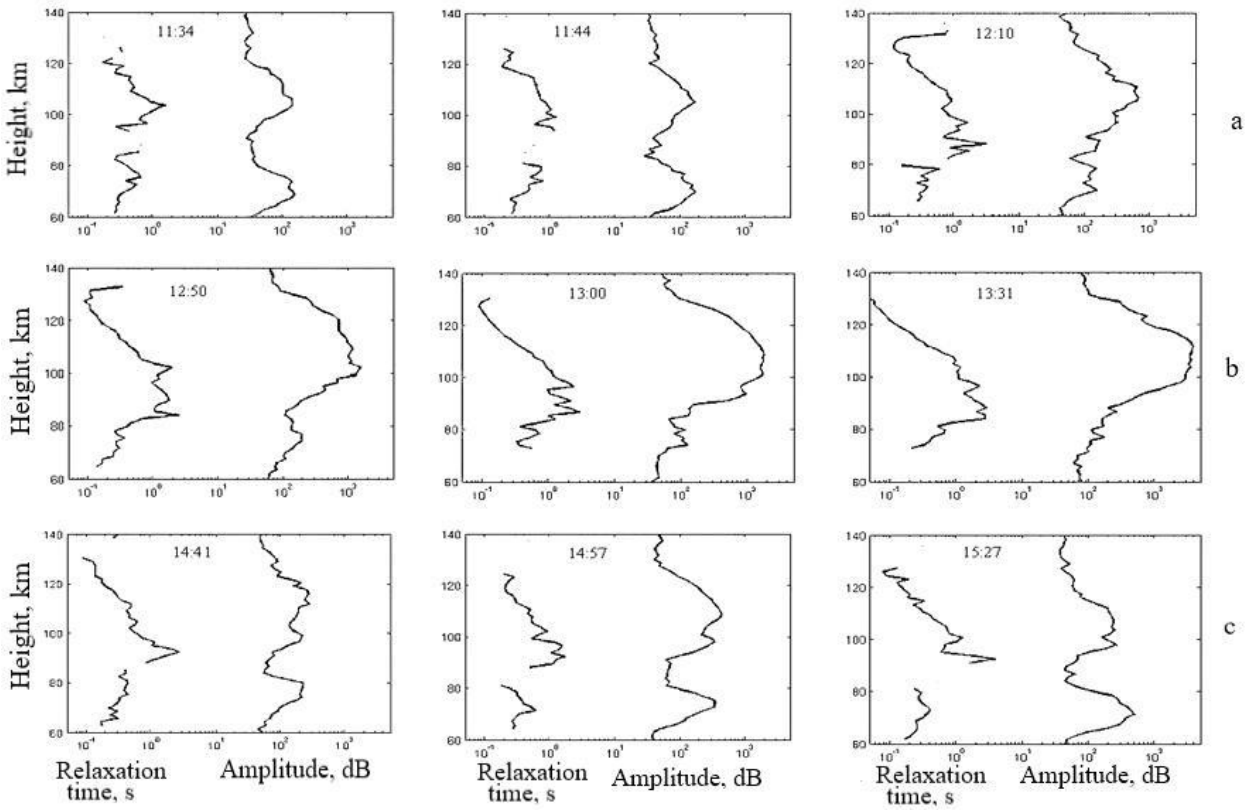

Figure 6. Vertical profiles of amplitude (right curves in the panels) and relaxation time (left curves) of a scattered signal during the March 20, 2015 eclipse: before the eclipse (*a*); near the maximum phase (*b*), and after the end of the eclipse (*c*), obtained by averaging over a 5-min interval. During the eclipse, there was an increase in the scattered signal amplitude in the E layer and its relaxation time in the D-region

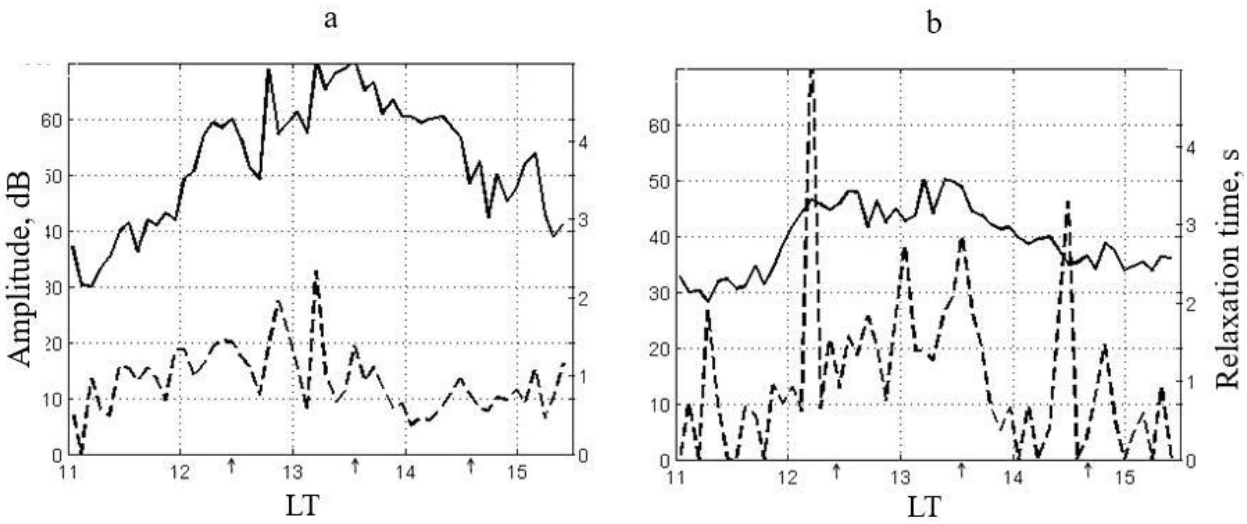

Figure 7. TIme dependences of scattered signal amplitude (solid line) and relaxation time (dashed line) for virtual heights of 88 km (*a*) and 100 km (*b*) during the March 20, 2015 partial solar eclipse. Phases of the eclipse are indicated by arrows. A significant increase is seen in the scattered signal amplitude during the eclipse, which in the E-region was 30–40 dB of the level of the beginning of observations and 20–30 dB directly during the eclipse

Presumably, there are several reasons for the appearance of this rarely observed signal. One of them may be the occurrence of a mesospheric summer echo due to a decrease in neutral atmosphere temperature (see below). Mesospheric summer echoes occur much less frequently at midlatitudes than in the polar regions. We can refer to [Thomas et al., 1992; Karashtin et al., 1997 and references therein]. Belikovich et al. [2003b] report on the first simultaneous observations of the summer mesosphere on August 13, 1999, i.e. a day after the partial solar eclipse with dual-frequency sounding at frequencies of 2.95 MHz and 9.9 MHz with a height resolution of ~3 km. In these experiments, mesospheric radio echoes were recorded from 75–85 km.

Another possible reason is related to the weakening of the influence of atomic oxygen on API formation above 80 km. According to the theory of API formation, the absence of a scattered signal in the upper part of the D-region, which generally takes place in experiments on generation of APIs, is due to the breakdown of the mechanism of their formation owing to an increase in the atomic oxygen density. It has been shown [Belikovich et al., 1999a, b; Belikovich et al., 2002] that quasi-periodic irregularities are formed in the D-region due to the electron temperature dependence of the coefficient of electron attachment to oxygen molecule. As the temperature rises, the attachment coefficient increases, which leads to a decrease in N_e in standing wave antinodes and to an increase in the negative ion density. During the eclipse, the D-region structure can change significantly since the rates of electron detachment from ions change. An increase in the scattered signal relaxation time 1.5–2 times during the eclipse can be explained by a corresponding decrease in the rate of electron detachment from molecular oxygen ions [Belikovich et al., 1999b; Belikovich et al., 2002]. This process for sunset and sunrise periods has been simulated in [Belikovich et al., 2000; Belikovich, Benediktov, 2002]. A similar process occurs during an eclipse. Bakhmetieva et al. [2020] have used the height dependence of the scattered signal relaxation time to find the lower boundary of occurrence of atomic oxygen. For March 20, 2015, this height varied from 80 to 84 km before and after the eclipse. During the eclipse, APIs were observed almost throughout the D-region.

Variations in the neutral atmosphere temperature and the plasma velocity

The method of determining the neutral component temperature and density, developed on the basis of API generation, provides data on these parameters at 90–130 km heights of the lower thermosphere, and the velocity is measured from 60 km [Belikovich et al., 1999b; Tolmacheva, Belikovich, 2004; Bakhmetieva, Zhemyakov, 2022]. Figure 8, *a* illustrates time dependences of temperature and density at a height of 100 km during the March 20, 2015 partial solar eclipse. There are deep variations in temperature and its decrease during the eclipse, when it went down by an average of 100 K and recovered to its previous level by the time the eclipse ended, experiencing deep quasi-periodic variations. Notice also the high correlation of the neutral component temperature and density variations.

Unlike Figure 5 in which the vertical velocity is given in height–time coordinates, Figure 8, *b* shows velocity variations at heights of 100, 110, and 115 km. The vertical velocity constantly varied in magnitude and direction, with characteristic deep velocity variations from –3 to +3 m/s (positive velocities correspond to downward motion). The velocity variations are seen to increase and reach their highest peak-to-peak amplitude near the maximum phase of the eclipse. Especially deep velocity variations from –8 to +6 m/s with periods 15–60 min were observed at 100 and 110 km. At 100 km, the velocity increased and changed direction, which could ensure plasma redistribution and formation of the E_s layer due to redistribution of ions in the geomagnetic field with regard to the inhomogeneous wind [Gershman, 1974; Whitehead, 1989; Mathews, 1998]. These features are also demonstrated in Figure 5. Thus, during the eclipse, wave motions with periods typical of IGWs manifested themselves in variations of the scattered signal characteristics — vertical plasma velocity, neutral component temperature and density.

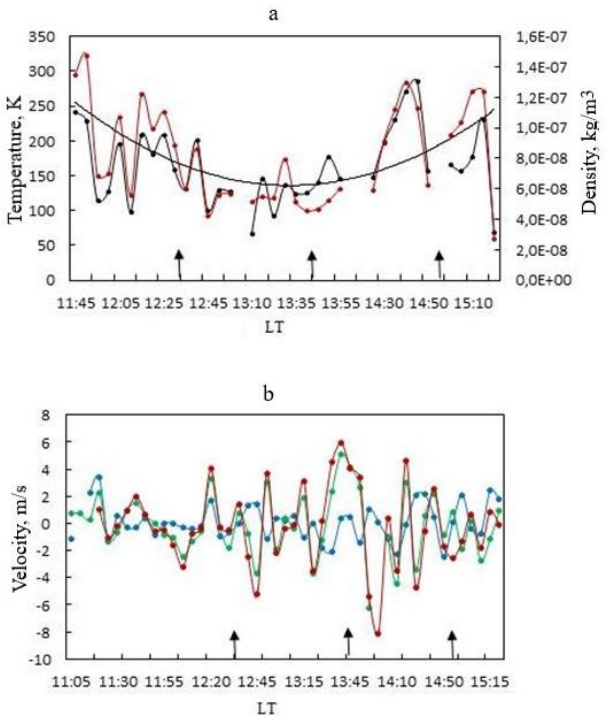

Figure 8. Variations in temperature (red dots), density of the neutral atmosphere (black) at a height of 100 km, and the second-order polynomial trend that provides information on mean temperature changes (*a*); vertical plasma velocity (*b*) at a height of 100 (red dots), 110 (dark blue), and 115 km (green dots) during the March 20, 2015 partial solar eclipse [Bakhmetieva et al., 2020]

The October 25, 2022 eclipse

The October 25, 2022 partial solar eclipse occurred from 12:30 to 14:57 LT with a maximum phase of 0.757 at 13:44 Moscow time (LT=UT+3) at high solar activity and under quiet geomagnetic conditions. The ionosphere was studied by the method of resonance scattering of radio waves by APIs on October 24–26 from 10 to 17 LT. According to ionosonde data, f_oE=2.2÷3.0, f_oF1=8.0÷9.0, and f_oF2=9.0÷10.8 MHz at high solar activity. There were type h and c E_s layers with a maximum reflection frequency to 3.5 MHz. During the eclipse, f_oF decreased by 3 MHz, from 10.8 to 7.8 MHz. A decrease in f_oE was no more than 1 MHz. Before the eclipse, on October 24, 2022, an E_s layer with f_oE_s to 7 MHz, which sometimes completely shielded the F layer, was recorded by the API method and in ionograms for several hours. The ionograms were taken by CADI every 5 min. There was a high noise level on that day. Contrary to previous years, the quasi-continuous heating of the ionosphere was used to generate APIs, and a scattered signal was received not only during relaxation of the irregularities, but during their development as well (see Figure 1).

Figure 9 displays the height-time dependence of scattered signal amplitude for the October 25, 2022 eclipse. The range of heights from the D-region to the F layer inclusive is covered. The probe waves of ordinary and extraordinary components specularly reflected from the F layer can be seen at 220–260 km. The signals scattered by APIs were observed at 65–85 km in the D-region and at 90–140 km in the E layer. From 100–110 km, a scattered signal from APIs in the E_s layer was received almost all day. During the measurements, the amplification level of the receiving equipment was mistakenly selected which provided a high level of the receiving signal from the F layer, but insufficient for good recording of scattered signals in the lower ionosphere. As a result, features of signal variations mainly in the F layer are clearly seen in this representation in Figure 9. Note the unusual dynamics of the virtual reflection height of the probe radio wave in the F layer. The relatively fast, approximately 5-min, and deep variations in height during the eclipse were replaced by slow, more typical of the quiet ionosphere.

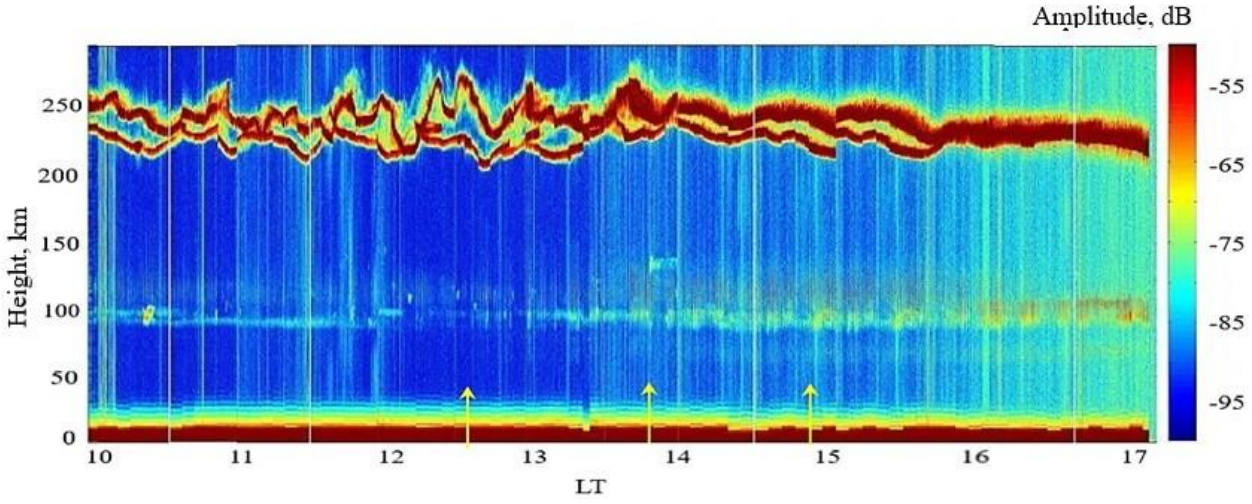

Figure 9. Height-time dependence of scattered signal amplitude in the October 25, 2022 eclipse during the development and relaxation of irregularities. Shown here are signals scattered by APIs in the D-region at heights 70–85 km, in the E layer at 90–140 km. The probe waves of ordinary and extraordinary components specularly reflected from the F layer are seen in the altitude range 220–260 km

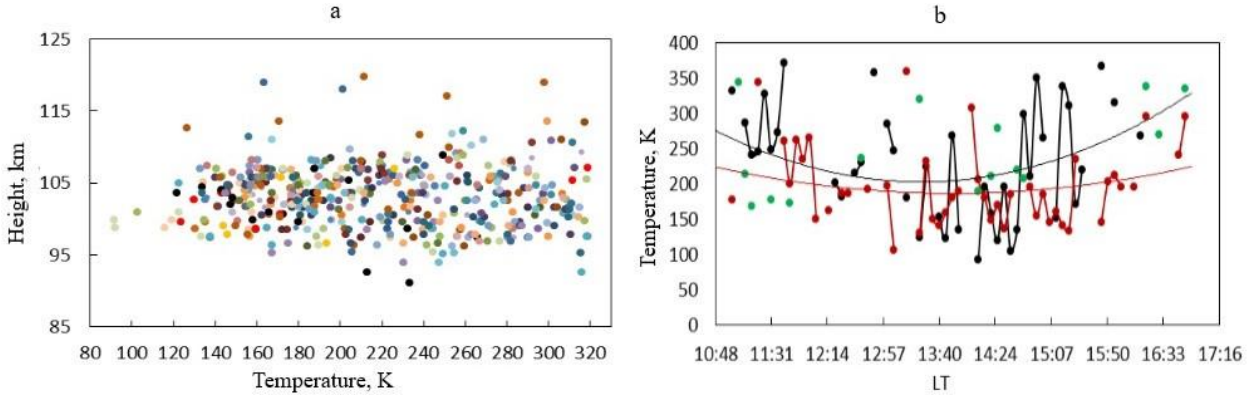

Figure 10. The neutral component temperature as measured from 10:00 to 17:00 on the day of the eclipse on October 25, 2022 at 90–120 km (*a*); temperature at 99.7 (black dots), 102.7 (red dots), and 107.3 km (green dots) (*b*). Solid lines indicate second-order polynomial trends for the first two heights

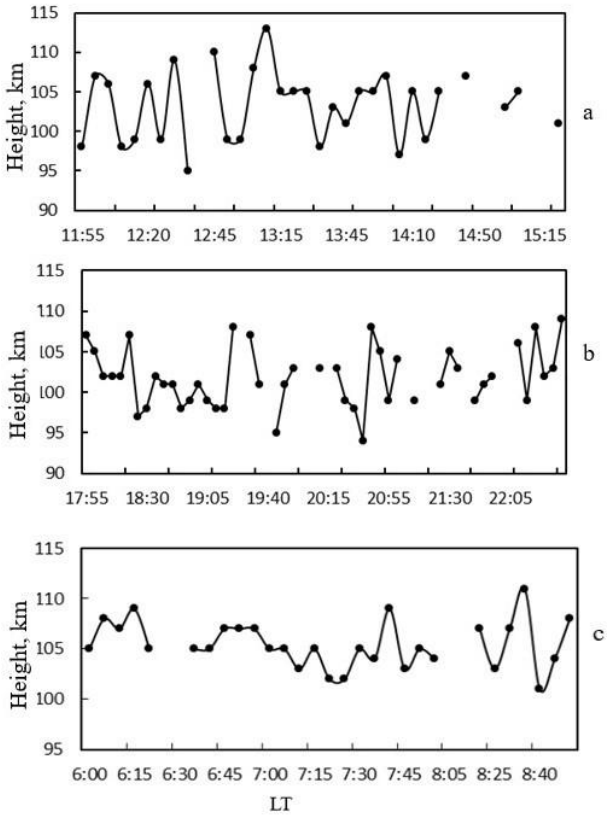

Figure 11. Turbopause level during the March 20, 2015 eclipse (*a*), at sunset and sunrise on August 12–13, 2015 (*b*, *c*)

Temperature of the neutral component, vertical velocity, turbulence characteristics

Temperature variations on the day of the eclipse are shown in Figure 10, *a*, where all temperature values are given without separating by heights. The point cloud provides insight into temperature variation limits and per day spread. It turned out that the highest cloud density was at 97–107 km, whereas the temperature varied from ~100 to 300 K. On the average, this is consistent with the results of our measurements by the API method [Belikovich et al., 1999b; Belikovich et al., 2002; Bakhmetieva et al., 2023] and other methods [Zherebtsov et al., 2020]. panel, *b* illustrates temperature variations at 99.7, 102.7, and 107.3 km; for the first two heights, second-order polynomial trends are plotted. Despite the relatively large temperature variations, it is obvious that its decrease correlates with the eclipse. The temperature dropped, on average, by 50–70 K at 99.7 km and by 20 K at 102.7 km. With the general tendency for the temperature to decrease at 107.3 km, there is not enough data to make such estimates.

Note that the temperature of the lower thermosphere depends on many natural factors such as atmospheric turbulence. Bakhmetieva et al. [2021] present information on changes in the turbopause level, obtained from measurements of scattered signal characteristics under different ionospheric conditions. The turbopause level is shown to vary significantly in height from 90 to 110–115 km. Figure 11 exemplifies changes in the turbopause level. Turbulence hinders the determination of temperature, reducing the relaxation time of irregularities, as compared to the diffusion relaxation time in the lower thermosphere, and increasing the measurement error. Such sessions are generally excluded from processing, but it is hardly possible to completely exclude the influence of turbulence. Note also that the turbulent velocity under disturbed conditions can increase from 2–3 to 5–7 m/s and is comparable in magnitude to the regular vertical velocity [Bakhmetieva et al., 2021; Bakhmetieva et al., 2023].

Features of the dynamic restructuring of the lower ionosphere on the day of the eclipse are represented by vertical plasma velocity profiles whose typical examples are given in Figure 12. The most significant altitude variations in velocity magnitude and direction were observed before the eclipse in the E layer at 90–110 km and in the D-region below 80 km. The height variation in velocity is characterized by a constant change of its magnitude and direction. Panel *a* exemplifies the profile only with downward velocity (all velocity values are positive) and its wave-like variations with height — both small-scale with a height scale 3–5 km and larger-scale ~25–30 km. Panels *b*, *c* show a variable velocity direction with a change of upward motion below 90 (100) km to downward, and a quasi-wave profile with a scale ~25–30 km. Under such conditions at these heights,

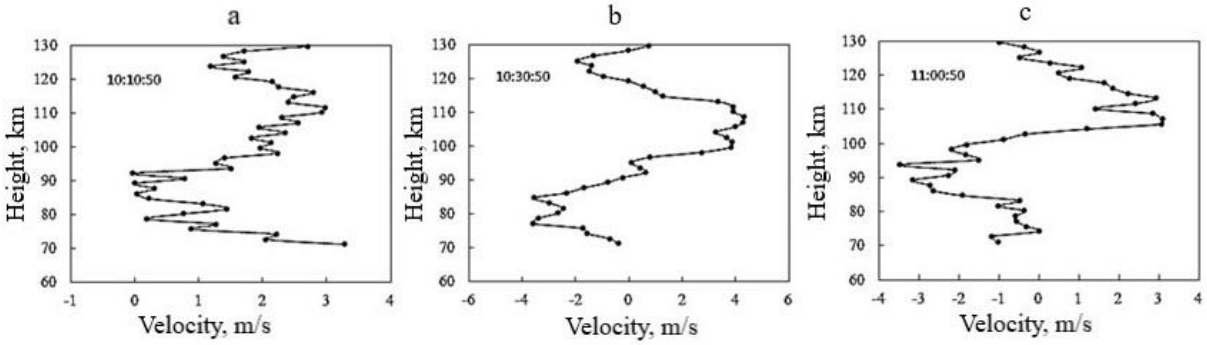

Figure 12. Height profiles of vertical plasma velocity for three sessions during the October 25, 2022 eclipse. Each point was obtained by 5-min averaging of initial data

Table 2

Date	*W*	*F*10.7	K_p	A_p
Aug. 16–17, 2000	167–174	1631	3.4	8
June 15–16, 2001	122–95	1673	1+; 2–	7
Aug. 12–13, 2015	40–48	65	3+; 4+	10, 12; 32
June 28–29, 2023	97–82	1501	2+; 3+; 3	7; 9; 15
Oct. 04–05, 2023	105–94	1544	2+	8

according to the theory of wind shear, there is a high probability of E_s-layer formation [Gershman, 1974; Whitehead, 1989; Mathews, 1998]. At the same heights, E_s layers were found in the height-time recording of the scattered signal amplitude and in the vertical sounding ionogram.

3. THE LOWER IONOSPHERE AT SUNSET AND SUNRISE

Studies of the lower ionosphere by the API method during solar eclipses and at sunset and sunrise, some results of which are presented in [Bakhmetieva et al., 2001, 2005; Belikovich et al., 1999b; Belikovich et al., 2002; Bakhmetieva, Grigoriev, 2022], have shown that the ionospheric processes occurring during these time periods are similar. Let us briefly delve into the features of the sunset-sunrise restructuring of the ionosphere. Table 2 provides information about the experiments performed, lists dates and heliogeophysical parameters during this period: sunspot number *W*, radio emission flux *F*10.7, geomagnetic indices K_p and A_p [http://www.wdcb.ru/stp/index.ru.html].

Except for August 2015, all other experiments were carried out during years of high solar activity. In August 2000 and August 2015, minor geomagnetic disturbances occurred with daily average K_p=3÷4.

Figure 13, *a*, *b* illustrates height-time dependences of the amplitude of a signal scattered by API, obtained during sunset-sunrise hours on June 15–16, 2001 and August 12–13, 2015. In both cases, at night the operation of the SURA facility stopped for a while when f_oF2 decreased and became lower than the operating frequency.

We can see almost complete similarity between the height and time dependences of the signal amplitude in June 2001 and August 2015: scattered signals in the D-region, E layer, and descending E_s layers modulated by atmospheric waves. Stratification of scattered signal amplitudes in the D-region similar to those shown in Figures 2 and 5 was observed.

It is well known that the D-region varies greatly during sunrise and sunset [Verronen et al., 2006; Baumann, 2022]. Figure 13, *a* shows that in the D-region an evening decrease in signal amplitude occurs when the zenith angle of the Sun changes from 90° to 105°. In the morning, the amplitude increases when the zenith angle of the Sun decreases from 97° to 90°. This is accompanied by an obvious asymmetry of the lower ionosphere at sunrise and sunset, which is manifested in the fact that in the evening scattered signals have a higher amplitude and occupy a wider height interval than at sunrise. In the evening, weak signals from the upper part of the D-region existed for about an hour after sunset at these heights. A wider and deeper amplitude minimum formed between the D-region and the E layer during sunrise is clearly visible. These processes are well described by the model that includes negative ions of one type, O_2^-, which is discussed in [Belikovich et al., 2000; Belikovich, Benediktov, 2002], where it is indicated that this model can be used to estimate densities of atomic oxygen and excited oxygen molecules in the 1Δg state. Also shown is a significant increase in the atomic oxygen density at sunrise [Belikovich et al., 1999b; Belikovich, Benediktov, 2002; Belikovich et al., 2002]. Similar signal amplitude variations in August 2015 were largely masked by a high noise level during sunset/sunrise hours.

Figure 13, *c* depicts height-time variations in vertical velocity with 5-min averaging during evening hours on August 12, 2015 and during morning hours on August 13, 2015. The velocity is represented as a color scale. In all the cases, the velocity varied from –8 to +8 m/s. There were deep and rapid velocity variations during morning hours on August 13, 2015. Evening hours on August 12, 2015 generally featured positive velocities in the D-region (downward motion) with a change of direction near 90 km. The periodic change of vertical velocity direction and magnitude with 15–20, 40–45, 60,

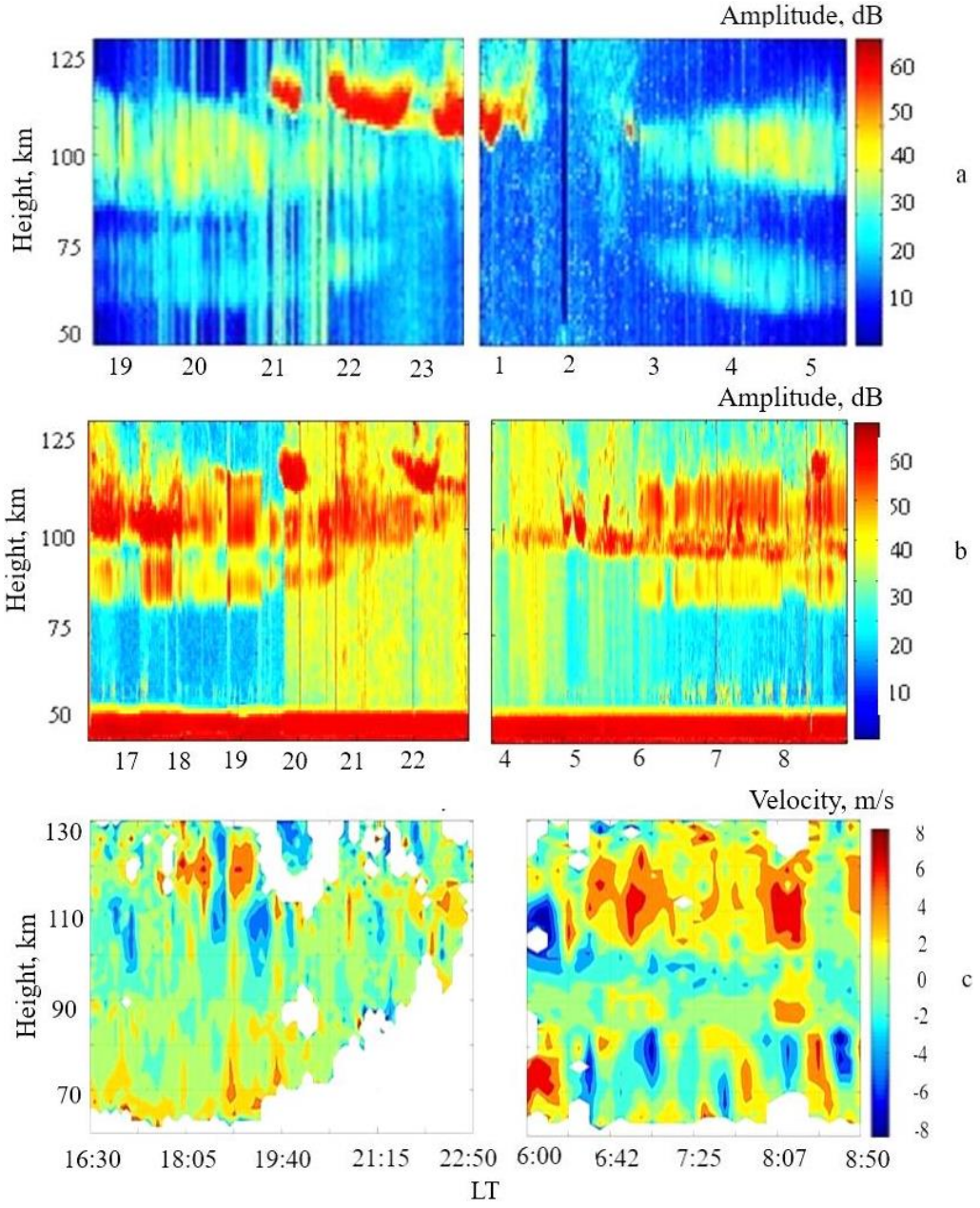

Figure 13. Height-time variations in scattered signal amplitude during sunset hours on June 15–16, 2001 (*a*) and August 12–13, 2015 (*b*); height-time variations in vertical velocity during sunset hours on August 12–13, 2015 (*c*)

120, 150, and 180 min wave variations is clearly seen. These periods are typical of IGWs propagating in Earth's atmosphere.

Tolmacheva, Belikovichn [2004] have examined vertical temperature and density profiles at heights between 90 and 110 km for evening hours on July 31, 2002 and morning hours on August 01, 2002, measured by the API method. In the temperature profile there was a minimum in the altitude range from 95 to 112 km. In the morning, the atmospheric density was 2.7 times higher than in the evening, and the temperature profile was shifted by several kilometers. The height of the minimum temperature in the evening and in the morning was 100 and 103 km respectively. The temperature near this height was almost the same (120–125 K). Comparing with data from the fall of 1990 [Tolmacheva, Belikovich, 2004; Belikovich et al., 1999b], when wave activity of the atmosphere was low, shows that the minimum temperature in the fall of 1990 was higher than in the summer of 2002 and amounted to ~140 K.

Thus, the studies of the lower ionosphere carried out by the API method have revealed a close similarity between variations in scattered signal amplitude, relaxation time, and vertical velocity during the eclipse and during sunset and sunrise hours.

CONCLUSION

We have presented the results of studies into the response of Earth's lower ionosphere to partial solar eclipses and at sunset and sunrise as observed in the Vasilsursk laboratory (56.13° N, 46.10° E) near Nizhny Novgorod.

Unique natural phenomena during the solar eclipse and on control days were investigated using the method of resonance scattering of radio waves by ionospheric plasma APIs, generated by powerful HF radio emission, and using the partial reflection technique based on radio wave scattering by natural irregularities of the D-region. APIs were generated by emission from SURA transmitters to the zenith of a powerful radio wave of extraordinary or ordinary polarization at frequencies of 4.3, 4.7, or 5.6 MHz. The transmitter for partial reflections operated at a frequency of 2.95 MHz; both magnetoionic components were received. We measured amplitudes and phases of signals scattered by natural and artificial irregularities. By measuring the scattered signal characteristics, we determined the neutral atmosphere temperature and density, the height of the turbopause, the turbulent velocity, and the regular vertical plasma velocity. We have drawn the following conclusions.

We have clearly shown that the conditions of the lower ionosphere during partial solar eclipses are similar to those during sunset and sunrise hours and are due to the fact that an actual decrease in solar radiation during an eclipse is analogous to the transition of the ionosphere to the dusk sector. During the development of eclipses and at sunset, an increase in heights of scattered signals in the D-region and the stratification of their amplitudes, characteristic of the transition to the nightside ionosphere, were observed. In the E layer, a 30–40 dB increase in amplitudes of signals scattered by irregularities, which was caused by a decrease in the absorption of high-power and probe waves, and an expansion of the altitude range of reception of scattered signals, i.e. altitudes of API formation, were recorded.

The API method was employed to determine the neutral atmosphere temperature at 90–130 km. The temperature was found to decrease on average by 50–70 K during eclipses. At the same time, the scattered signal amplitude increased by 30–40 dB; the relaxation time, 1.5–2.0 times. In some cases, the signal amplitude was stratified in the D-region due to stratification of the N_e profile. The turbulence of the lower ionosphere associated with propagation of atmospheric waves increased.

N_e measured by the PR technique in the D-region during the August 01, 2008 eclipse decreased 3–5 times. Above 88 km, the ionospheric response was delayed by 20–25 min with respect to the maximum phase of the eclipse, whereas in the lower part of the D-region this response delayed by no more than a few minutes.

During the eclipses, scattered signals with high amplitude and relatively long relaxation time were detected after the end of the impact on the ionosphere from mesopause heights (84–88 km). Scattered signals at these heights are usually absent due to an increase in the atomic oxygen density, which impede the generation of APIs owing to attachment of electrons to oxygen molecules during triple collisions. This allows us to assume that the atomic oxygen density during an eclipse at these heights decreases.

Intense wave motions with periods typical of IGWs were observed in vertical plasma velocity variations. The main features of the height-time variations in the vertical velocity in the lower ionosphere during observation of the solar eclipse and during sunset/sunrise hours are similar.

Comparing these variations with time variations in the vertical velocity, as well as with measurements of the vertical N_e profile, allows us to conclude that there was a significant change in both the ionized and neutral components of the atmosphere in the lower ionosphere during the eclipse.

The work was carried out under project No. FSWR-2023-0038 in the basic part of the Government assignment of the Ministry of Science and Higher Education of the Russian Federation. Experiments on generation of APIs by the SURA facility in 2022–2023 were financially supported by RSF (Grant No. 21-72-10131).

REFERENCES

Afraimovich E.L., Palamartchouk K.S., Perevalova N.P., Chernukhov V.V., Lukhnev A.V., Zalutsky V.T. Ionospheric effects of the solar eclipse of March 9, 1997, as deduced from GPS data. *Geophys. Res. Lett.* 1998, vol. 25, no. 4, pp. 465–469.

Afraimovich E.L., Kosogorov E.A., Lesyuta O.S., Yakovets A.F., Ushakov I.I. Geomagnetic control of the spectrum of traveling ionospheric disturbances based on data from a global GPS network. *Ann. Geophys*., 2001, vol. 19, no 7, pp. 723–731.

Akimov L.A., Grigorenko E.I., Taran V.I., Tyrnov O.F., Chernogor L.F. Integrated radiophysical and optical studies of dynamical processes in the atmosphere and geospace caused by the solar eclipse of August 11, 1999. *Usp. Sovr. Radioelektron*. 2002, no. 2, pp. 25–63.

Artem'eva G.M., Belikovich V.V., Benediktov E.A., Erukhimov L.M., Korobkov Yu.S. Measurements of the absorption of cosmic radio emission during the solar eclipse of February 15, 1961. *Geomagnetism and Aeronomy*. 1962, vol. 2, no. 1, pp. 58–60.

Babakhanov I.Y., Belinskaya A.Y., Bizin M.A., Grekhov O.M., Khomutov S.V., Kuznetsov V.V., Pavlov A.F. The geophysical disturbance during the total eclipse of the 1 August 2008 in Novosibirsk, Russia. *J. Atmos. Solar-Terr. Phys*. 2013, vol. 92, pp. 1–6.

Bamford R.A. The effect of the 1999 total solar eclipse on the ionosphere. *Phys. Chem. Earth (C)*. 2001, vol. 26, no. 5, pp. 373–377. DOI: 10.1016/S1464-1917(01)00016-2.

Barad R.K., Sripathi S., England S.L. Multi-instrument observations of the ionospheric response to the 26 December 2019 solar eclipse over Indian and Southeast Asian longitudes. *J. Geophys. Res.: Space Phys*. 2022, vol. 127, e2022JA030330. DOI: 10.1029/2022JA030330.

Bakhmetieva N.V., Grigoriev G.I. Study of the Mesosphere and Lower Thermosphere by the Method of Creating Artificial Periodic Irregularities of the Ionospheric Plasma. *Atmosphere*. 2022, vol. 13, 1346. DOI: 10.3390/atmos13091346.

Bakhmetieva N.V., Zhemyakov I.N. Vertical plasma motions in the dynamics of the mesosphere and lower thermosphere of the Earth. *Russian Journal of Physical Chemistry B.* 2022, vol. 16, no 5, pp. 990–1007. DOI: 10.1134/s1990793122050177.

Bakhmetieva N.V., Belikovich V.V., Benediktov E.A., Tolmacheva A.V. Studies of the irregular structure of the ionosphere using scattering of radio waves on artificial periodic inhomogeneities. *Radiophysics and Quantum Electronics.* 2001, vol. 44, no. 12, pp. 924–934.

Bakhmet'eva N.V., Belikovich V.V., Kagan L.M., Ponyatov A.A. Sunset-sunrise characteristics of sporadic layers of ionization in the lower ionosphere observed by the method of

resonance scattering of radio waves from artificial periodic inhomogeneities of the ionospheric plasma . *Radiophysics and Quantum Electronics.* 2005, vol. 48, no 1, pp. 14–28. DOI: 10.1007/s11141-005-0044-3.

Bakhmet'eva N.V., Belikovich V.V., Egerev M.N., Tolmacheva A.V. Artificial periodic irregularities, wave phenomena in the lower ionosphere, and the sporadic E layer. *Radiophysics and Quantum Electronics*. 2010, vol. 53, pp. 69–81. DOI: 10.1007/s11141-010-9210-3.

Bakhmet'eva N.V., Bubukina V.N., Vyakhirev V.D., Kalinina E.E., Komrakov G.P. Response of the lower ionosphere to the partial solar eclipses of August 1, 2008 and March 20, 2015 based on observations of radio-wave scattering by the ionospheric plasma irregularities. *Radiophysics and Quantum Electronics.* 2016, vol. 59, pp. 782–793. DOI: 10.1007/s11141-017-9747-5.

Bakhmetieva N.V., Vyakhirev V.D., Kalinina E.E., Komrakov G.P. Earth's lower ionosphere during partial solar eclipses according to observations near Nizhny Novgorod. *Geomagnetism and Aeronomy.* 2017, vol. 57, no. 1, pp. 58–71. DOI: 10.1134/S0016793217010029.

Bakhmetieva N.V., Kulikov Y.Y., Zhemyakov I.N. Mesosphere ozone and the lower ionosphere under plasma disturbance by powerful high-frequency radio emission. *Atmosphere*. 2020, vol. 11, iss. 11, p. 1154.

Bakhmetieva N.V., Grigoriev G.I., Vinogradov G.R., Zhemyakov I.N., Kalinina E.E., Pershin A.V. Parameters of atmospheric turbulence and dynamics of the lower ionosphere in research at the SURA facility. *Geomagnetism and Aeronomy*. 2021, vol. 61, no. 6, pp. 871–887. DOI: 10.1134/S0016793221060025.

Bakhmetieva N.V., Zhemyakov I.N., Grigoriev G.I., Kalinina E.E. Impact of natural factors on the temperature in the lower thermosphere. *Russ. J. Phys. Chem. B.* 2023, vol. 17, pp. 1202–1215.

Baumann C., Kero A., Raizada S., Rapp M., Sulzer M.P., Verronen P.T., Vierinen J. Arecibo measurements of D-region electron densities during sunset and sunrise: implications for atmospheric composition. *Ann. Geophys.* 2022, vol. 40, pp. 519–530. DOI: 10.5194/angeo-40-519-2022.

Belikovich V.V., Benediktov E.A. Lower part of the D region of the ionosphere using artificial periodic inhomogeneities. *Radiophys Quantum Electron*. 1986, vol. 29, pp. 963–973. DOI: 10.1007/BF01034133.

Belikovich V.V., Benediktov E.A. Study of the twilight D region of the ionosphere using artificial periodic inhomogeneities. *Radiophysics and Quantum Electronics.* 2002, vol. 45, no 6, pp. 458–464.

Belikovich V.V., Goncharov N.P. Study of the ionospheric D-region with the help of artificial periodic irregularities. *Geomagnetism and Aeronomy.* 1994, vol. 34, no. 6, pp. 84–95.

Belikovich V.V., Benediktov E.A., Terina G.I. Diagnostics of the lower ionosphere by the method of resonance scattering of radio waves. *J. Atmos. Terr. Phys.*1986, vol. 48, no. 11-12, pp. 1247–1253.

Belikovich V.V., Benediktov E.A., Bubukina V.N., Vyakhirev V.D. Artificial periodic inhomogeneities and a model for the lower part of the D region. *Radiophys Quantum Electron.* 1999a, vol. 42, no 5, pp. 382–387. DOI: 10.1007/BF02677617.

Belikovich V.V., Benediktov E.A., Tolmacheva A.V., Bakhmetieva N.V. *Issledovanie ionosfery s pomoshch'yu iskusstvennykh periodicheskikh neodnorodnostei* [Study of the ionosphere using artificial periodic irregularities]. Nizhny Novgorod, IAP RAS Publ., 1999b, 155 p. (In Russian).

Belikovich V.V., Benediktov E.A., Trunov D.V. Height profiles of the amplitude and relaxation time of artificial periodic irregularities in the D-region. *Geomagnetism and Aeronomy*. 2000, vol. 40, pp. 733–738.

Belikovich V.V., Benediktov E.A., Tolmacheva A.V., Bakhmet'eva N.V. *Ionospheric Research by Means of Artificial Periodic Irregularities* – Copernicus GmbH, Katlenburg-Lindau, Germany. 2002, 160 p.

Belikovich V.V., Vyakhirev V.D., Kalinina E.E., Tereshshenko V.D., Ogloblina O.F., Tereshshenko V.A. Study of the ionospheric D-region using partial reflections at the middle latitudes and in the auroral zone. *Radiophysics and Quantum Electronics.* 2003a, vol. 46, no. 3, pp. 162–171.

Belikovich V.V., Karashtin A.N., Komrakov G.P., Shlyugaev Y.V. Simultaneous MF and HF radio sounding of the midlatitude mesosphere. *Geomagnetism and Aeronomy*. 2003b, vol. 43, no. 1, pp. 96–100.

Belikovich V.V., Vyakhirev V.D., Kalinina E.E., Tereshchenko V.D., Chernyakov S.M., Tereshchenko V.A. Ionospheric response to the partial solar eclipse of March 29, 2006, according to the observations at Nizhny Novgorod and Murmansk. *Geomagnetism and Aeronomy.* 2008, vol. 48, no. 1, pp. 98–103. DOI: 10.1134/s0016793208010118.

Benediktov E.A., Vyakhirev V.D., Goncharov N.P., Grishkevich L.V., Ivanova V.A. Variations in electron concentration of the ionospheric D-region, *Radiophysics and Quantum Electronics*. 1978, vol. 21, no. 3, pp. 348–351. (In Russian).

Bischoff K., Taubenheim J. A study of ionospheric pulse absorption (A1) on the 4 Mc/s during the solar eclipse of May 20, 1966. *J. Atmos. Terr. Phys.* 1967, vol. 29, no. 9, pp. 1063−1069. DOI: 10.1016/0021-9169(67)90140-7.

Brunelli B.E., Namgaladze A.A. Physics of the ionosphere. M.: Nauka, 1988, 528 p. (In Russian).

Chandra H., Sharma Som, Lele P.D., Rajaram G., Arun Hanchinal. Ionospheric measurements during the total solar eclipse of 11 August 1999. *Earth Planets Space*. 2007, vol. 59, pp. 59−64. DOI: 10.1186/BF03352023.

Cherniak I., Zakharenkova I. Ionospheric total electron content response to the great American solar eclipse of 21 August 2017. *Geophys. Res. Lett.* 2018, vol. 45, no. 3, pp. 1199–1208. DOI: 10.1002/2017GL075989.

Chernogor L.F. *Fizicheskie effekty solnechnykh zatmenii v atmosphere I geokosmose* [Physical effects of solar eclipses in the atmosphere and geospace]. Kharkov: Publishing House of the Kharkov National University, 2013, 480 p. (In Russian).

Gershman B.N. *Dynamics of the Ionospheric Plasma*. Moscow, Nauka, 1974, 256 p. (In Russian).

Gershman B.N., Ignatiev Yu.A., Kamenetskaya G.Kh. *Mechanisms of formation of the ionospheric sporadic layer at different latitudes.* Moscow, Nauka, 1978, 108 p. (In Russian).

Dang T., Lei J., Wang W., Zhang B., Burns A., Le H., et al. Global responses of the coupled thermosphere and ionosphere system to the August 2017 Great American Solar Eclipse. *J. Geophys. Res.: Space Phys.* 2018, vol. 123, no 5, pp. 7040–7050. DOI: 10.1029/2018JA025566.

Danilkin N.P., Kochenova N.A., Svechnikov A.M. The ionospheric state over Rostov-on-Don during the solar eclipse of February 15, 1961. *Geomagnetism and Aeronomy*. 1961, vol. 1, no. 4, pp. 612–615. (In Russian).

Farges T., Le Pichon A., Blanc E., Perez S., Alcoverro B. Response of the lower atmosphere and the ionosphere to the eclipse of August 11, 1999. *J. Atmos. Solar-Terr. Phys.* 2003, vol. 65, no 6, pp. 717–726. DOI: 10.1016/S1364-6826(03)00078-6.

Huijun Le, Libo Liu, Xinan Yue, Weixing Wan, Baiqi Ning. Latitudinal dependence of the ionospheric response to solar eclipses. *J. Geophys. Res.: Space Phys.* 2009, vol. 114, iss. A7. DOI: 10.1029/2009JA014072.

Ivanov V.A., Ivanov D.V., Ryabova N.V., Ryabova M.I. Study of the specific features of HF signal propagation on inclined and NVIS radio lines during solar eclipses. Vestn. Nizhegorodskogo Univ. im. N.I. Lobachevskogo. 2012, no. 2, pp. 59–65. (In Russian).

Kagan L.M., Nicolls M.J., Kelley M.C., Carlson H.C., Belikovich V.V., Bakhmet'eva N.V., et al. Observation of radiowave-induced red hydroxyl emission at low altitude in the ionosphere. *Phys. Rev. Lett.* 2005, vol. 94, 095004.

Kovalev A.A., Kolesnik A.G., Kolesnik S.A., Kolmakov A.A. Ionospheric effects of solar eclipses at midlatitudes. *Geomagnetism and Aeronomy*. 2009, vol. 49, pp. 476–482. DOI: 10.1134/S0016793209040070.

Kane J.A. D-region electron density measurements during the solar eclipse of May 20, 1966. *Planet. Space Sci.* 1969, vol. 17, no. 4, pp. 609–616. DOI: 10.1016/0032-0633(69)90183-4.

Karashtin A.N., Shlyugaev Y.V., Abramov V.I., Belov I.F., Berezin I.V., Bychkov V.V., et al. First HF radar measurements of summer mesopause echoes at SURA. *Ann. Geophys.* 1997, vol. 15, no. 7, pp. 935–941.

Klimenko V.V., Bessarab F.S., Korenkov Y.N. Numerical simulation of effects of the August 11, 1999 solar eclipse in the outer ionosphere. *Cosmic. Res.* 2007, vol. 45, pp. 102–109. DOI: 10.1134/S0010952507020037.

Lei J., Dang T., Wang W., Burns A., Zhang B., Le H. Long-lasting response of the global thermosphere and ionosphere to the 21 August 2017 solar eclipse. *J. Geophys. Res.: Space Phys.* 2018, vol. 123, no. 5, pp. 4309–4316. DOI: 10.1029/2018JA025460.

Ladynin A.V., Semakov N.N., Khomutov S.Yu. Changes in the daily geomagnetic variation during the total solar eclipse on August 1, 2008. *Russian Geology and Geophysics*. 2011, vol. 52, no. 3, pp. 347–356. DOI: 10.1016/j.rgg.2011.02.007.

Madhav Haridas M.K., Manju G. On the response of the ionospheric F region over Indian low-latitude station Gadanki to the annular solar eclipse of 15 January 2010. *J. Geophys. Res.* 2012, vol. 117, A01302. DOI: 10.1029/2011JA016695.

MacPherson B., Gonzales S.A., Sulzer M.P., Bailey G.J., Djuth F., Rodriguez P. Measurements of the topside ionosphere over Arecibo during the total solar eclipse of February 26, 1998. *J. Geophys. Res*. 2000, vol. 105, no. 10, pp. 23055–23067. DOI: 10.1029/2000JA000145.

Manju G., Sridharan R., Ravindran Sudha, Madhav Haridas M.K., Tarun K. Pant, Sreelatha P., Mohan Kumar S.V. Rocket born in-situ electron density and neutral wind measurements in the equatorial ionosphere — Results from the January 2010 annual solar campaign from India. *J. Atmos. Terr. Phys.* 2012, vol. 86, pp. 56–64. DOI: 10.1016/j.jastp.2012.06.009.

Mathews J.D. Sporadic E: current views and recent progress. *J. Atmos. Terr. Phys.* 1998, vol. 60, no. 4, pp. 413–435.

Panasenko S.V., Yuichi Otsuka, Max van de Kamp, Chernogor L.F., Shinbori A., Tsugawa T., Nishioka M. Observation and characterization of traveling ionospheric disturbances induced by solar eclipse of 20 March 2015 using incoherent scatter radars and GPS networks. *J. Atmos. Solar–Terr. Phys.* 2019, vol. 191, 105051. DOI: 10.1016/j.jastp.2019.05.015.

Rishbeth H. Solar eclipses and ionospheric theory. *Space Sci. Rev*. 1968, vol. 8, no. 4, pp. 543–544.

Salah J.F., Oliver W.L., Foster J.C., Holt J.M., Emery B.A., Roble R.G. Observations of the May 30, 1984, annular solar eclipse at Millstone Hill. *J. Geophys. Res.* 1986, vol. 91, no. A2, pp. 1651–1660. DOI: 10.1029/JA091iA02p01651.

Sneva Y., Rupesh M.D., Dabas R.S., Gwal A.K. The response of sporadic E-layer to the total solar eclipse of July 22, 2009 over the equatorial ionization anomaly region of the Indian zone. *Adv. Space Res*. 2013, vol. 51, pp. 2043–2047.

Tereshchenko V.D., Vasil'ev E.B., Yakimov M.V., Tereshchenko V.A., Ogloblina O.F., Tarichenko A.M. Radar observations over the lower polar ionosphere during the partial solar eclipse of August 11, 1999. *Radiolokatsionnoe issledovanie prirodnykh sred: Tr. XVI–XIX Vserossiiskikh simpoziumov* [Radar Studies of Natural Environments: Proc. XVI–XIX All-Russian Symposiums]. Saint Petersburg: VIKKA Publ., 2001, vol. 2, pp. 347–352. (In Russian).

Thomas L., Astin I., Prichard T. The characteristics of VHF echoes from the summer mesopause region at mid-latitudes. *J. Atmos. Terr. Phys.* 1992, vol. 54, pp. 969–977.

Tolmacheva A.V., Belikovich V.V. Measurements of the temperature and density of the upper atmosphere using artificial periodic irregularities during the summer seasons of 1999–2002. *Int. J. Geomagn. Aeron.* 2004, vol. 5, G11008. DOI: 10.1029/2004G1000061.

Tsai H.F., Liu J.Y. Ionospheric total electron contents response to solar eclipse. *J. Geophys. Res*. 1999, vol. 104, no. 6, pp. 12657–22668.

Uryadov V.P., Leonov A.M., Ponyatov A.A., Boiko G.N., Terent'ev S.P. Variations in the characteristics of a HF signal over an oblique sounding path during the solar eclipse on August 11, 1999. *Radiophysics and Quantum Electronics*. 2000, vol. 43, pp. 614–618. DOI: 10.1023/A:1004801201847.

Wang X., Berthelier J.J., Lebreton J.P. DEMETER observations during the March 29, 2006 solar eclipse. *Geophysical Research Abstracts*. 2008, vol. 10, EGU2008-A-06988.

Verronen P.T., Ulich Th., Turunen E., Rodger C.J. Sunset transition of negative charge in the D-region ionosphere during high-ionization conditions. *Ann. Geophys.* 2006, vol. 24, pp. 187–202. DOI: 10.5194/angeo-24-187-2006.

Vertogradov G.G., Vertogradova E.G., Uryadov V.P. The response of the ionosphere to the solar eclipse March 29, 2006 based on oblique LFM sounding data. *Heliogeophysical Research*. 2015, no. 11.

Whitehead J.D. Recent work on mid-latitude and equatorial sporadic-E. *J. Atmos. Terr. Phys.* 1989, vol. 51, no. 5, pp. 401–424. DOI: 10.1134/S1990793123050160.

Zherebtsov G.A., Perevalova N.P., Shpynev B.G., Medvedeva I.V., Ratovsy K.G., Khabituev D.S., Yasukevich A.S. Volnovye protsessy v atmosphere Zemli i ikh vliyanie na ionosferu [Wave Processes in the Earth's Atmosphere and Their Effects on the Ionosphere]. Moscow: GEOS Publ., 2020, 198 p.

URL: http://www.wdcb.ru/stp/index.ru.html (accessed March 22, 2024).

URLhttps://www.izmiran.ru/ionosphere/moscow/ (accessed March 22, 2024).

This paper is based on material presented at the 19th Annual Conference on Plasma Physics in the Solar System, February 5–9, 2024, IKI RAS, Moscow.

Original Russian version: Bakhmetieva N.V., Grigoriev G.I., Zhemyakov I.N., Kalinina E.E., Lisov A.A., published in Solnechno-zemnaya fizika. 2024. Vol. 10. No. 3. P. 129–145. DOI: 10.12737/szf-103202414.

How to cite this article

Bakhmetieva N.V., Grigoriev G.I., Zhemyakov I.N., Kalinina E.E., Lisov A.A. Features of Earth's lower ionosphere during solar eclipse and sunset and sunrise hours according to measurements by the API method near Nizhny Novgorod. *Solar-Terrestrial Physics*. 2024. Vol. 10. Iss. 3. P. 121–136. DOI: 10.12737/stp-103202414.